

## Development of nano-crosslinked polyacrylonitrile ions exchanger particles for dye removal: kinetic, isotherm, and thermodynamic studies

M.S. Mohy Eldin<sup>a,\*</sup>, Y.A. Aggour<sup>b</sup>, M.R. Elaassar<sup>a,c</sup>, G.E. Beghet<sup>b</sup>, R.R. Atta<sup>b</sup>

<sup>a</sup>Polymer Materials Research Department, Advanced Technology and New Materials Research Institute, City of Scientific Research and Technological Applications (SRTA-City), New Borg El-Arab City 21934, Alexandria, Egypt, Tel. +203 4593 414; emails: mmohyeldin@srtacity.sci.eg (M.S. Mohy Eldin), mohamed\_elaassar@yahoo.com (M.R. Elaassar)

<sup>b</sup>Physical Chemistry, Department of Chemistry, Faculty of Science at (New) Damietta, Damietta University, Egypt, Tel. +2057 2403866; emails: yassina9@yahoo.com (Y.A. Aggour), GamalBekheit@du.edu.eg (G.E. Beghet), ramadanatta75@du.edu.eg (R.R. Atta)

<sup>c</sup>Chemistry Department, College of Science, Jouf University, Sakaka 2014, Saudi Arabia

Received 12 January 2019; Accepted 16 September 2019

### ABSTRACT

Poly(acrylonitrile-co-divinylbenzene) nanoparticles (PAN) based adsorbents developed for the adsorption of methylene blue (MB) from contaminated water. Essential factors affecting the adsorption process such as MB concentration, adsorption time and adsorption temperatures have studied. A linear increment of the adsorption capacity recognized with the increase of the dye concentration up to 7 ppm, then leveling off was noticed. The adsorption capacity of both adsorbents increased linearly with adsorption time, and the equilibrium almost reached after 5 h. A negative impact of the adsorption temperature observed upon the adsorption capacity. Fitting the adsorption results with different kinetic models revealed that the adsorption of MB met with the pseudo-second-order kinetic model having higher  $R^2$  values; 0.9971 and 0.9945 for PAN and amidoxime modified polyacrylonitrile. Testing the diffusion mechanism of the MB adsorption process indicates that the film diffusion governs the rate-limiting process. The Freundlich isotherm model was found more favorable for the adsorption of MB. The thermodynamic parameters indicate the exothermic nature of the adsorption process. The best performance recognized at low temperatures.

**Keywords:** Polyacrylonitrile; Nanoparticles; Amidoxime; Methylene blue; Adsorption; Kinetic; Isotherm; Thermodynamic

### 1. Introduction

In the last century, industrialization was the driving force for development all over the world. To develop any society, a wide range of industries is participating, such as metallic, textile, mining, tannery, and plastic ones. As a result of such industrial activities, many wastes discharged in the water system with improper treatment. The most harmful discharged wastes are heavy metals and dyes, which caused recognized damages on both the environment and human-kind's life [1]. Different diseases have been monitored as

a result of heavy metals contamination [2] while environmental damages mainly caused by dyestuff [3].

The wastewater containing dyes is challenging to treat, since the dyes are recalcitrant organic molecules, resistant to aerobic digestion, and are stable to light, heat and oxidizing agents [4,5]. During the past three decades, several physicals, chemical and biological decolorization methods have reported; few, however, have been accepted by the paper and textile industries. Amongst the numerous techniques of dye removal, adsorption using different adsorbents is the procedure of choice. The adsorption technique gives the best results as it can be used to remove different types of coloring

\* Corresponding author.

materials [6–10]. High surface area adsorbents required to achieve high efficient adsorption process. Functionalized nano-materials show an estimated contribution in this direction, which removes metals ions and dyes through chelating and ions exchanging [11–16].

Hossain et al. [17] reviewed the diffusion of cationic dyes into poly(acrylonitrile-co-divinylbenzene) nanoparticles (PAN). Recently, Şuteu et al. [18] present new results about the efficiency of wastes based on hydrolyzed polyacrylonitrile textile fibers (HPAN) as sorbents in the removal of some dyes from textile effluents. The effect of some experimental variables, such as initial dye concentration, sorbent mass, pH, temperature, and contact time investigated.

The sorbent–dye sorption systems are described using Freundlich, Langmuir, and Dubinin–Radushkevitch isotherm models. The good removal of stains from aqueous medium using textile fibers wastes indicates the actual tendency of using non-conventional sorptive materials to reduce the overall cost of sorbent preparation. The surface area of the adsorbent materials is a determining factor. Nano adsorbents with the high surface area are the optimum choice to have an efficient adsorption process. PAN has been prepared using different techniques [19–22].

Due to the incorporation of nitrile groups in its structure, polyacrylonitrile materials of different physical forms have been produced, modified, and functionalized. Accordingly, the forming of hydrogen bonds and donor-acceptor complexes with positively charged species are the main benefits of using polyacrylonitrile-based adsorbents in the treatments of wastewaters polluted by heavy metals cations and cationic dyes [23].

In our previous studies, developed polyacrylonitrile nanoparticles have examined in the treatment of methylene blue (MB) contaminated wastewater [24,25]. Moreover, polyacrylonitrile grafted cotton fabrics used and the adsorption data analyzed with kinetic, isothermal, and thermodynamic models [26,27].

In the current study, the developed PAN adsorbents used in the treatment of MB synthetic aqueous solution and the adsorption data fitted with kinetic, isothermal, and thermodynamic models.

## 2. Materials and methods

### 2.1. Materials

The following analytical grade chemicals were purchased from commercial sources and used without further purification. Acrylonitrile (AN) (Aldrich, Germany, 99%). Divinylbenzene (DVB) (Aldrich, Germany, technical grade, 80%). Potassium persulfate (KPS) extra pure (Loba Chemie, Mumbai, India, 98%). Ethanol (EtOH) (Aldrich, Germany, 99.9%). Hydroxylamine hydrochloride (HA) (Adwic, Egypt, 97%). Sodium hydroxide (99%). Sodium chloride (NaCl) (99%) and MB (MB, 82%) purchased from Alpha Chemika, Mumbai, India. Distilled water employed in all reactions.

### 2.2. Preparation of the adsorbents nanoparticles

The PAN prepared by precipitation polymerization technique. In 0.01 M KPS solution (water: EtOH; 1:1) the monomers DVB and AN were dissolved to have 10% final

co-monomers concentration. The polymerization process conducted at 55°C for 4 h, then the copolymer was centrifuged at 8,000 rpm and washed with (Water/EtOH) solution to remove unreacted monomers and left to dry at 80°C before reacted with hydroxylamine. In 50 mL of 1% HA, 1 g of the copolymer was reacted at 60°C for 4 h to have the amidoxime modified Poly(acrylonitrile-co-divinylbenzene) (HP (AN-co-DVB)) particles. Then, treated with 30 mL of 2% NaOH solution at room temperature for 1 h. The modified copolymer particles were then successively washed with distilled water to remove the excess of NaOH and finally dried at 80°C for 24 h. [25]. A schematic diagram of the prepared copolymer and its modified counterpart presented in Fig. 1.

### 2.3. Preparation of basic dye solution

MB,  $C_{16}H_{18}N_3SCl \cdot 3H_2O$ , a stock solution prepared by dissolving 0.01 g of MB in 1,000 mL distilled water. The dye concentration measured at wavelength 660 nm using a spectrophotometer [25].

### 2.4. Batch MB adsorption experiments

The adsorption experiments were carried out in a batch process by using MB aqueous solution. The variable parameters namely; the initial MB concentration, the adsorbent amount, the contact time, and the adsorption temperature were studied. The MB adsorption studies performed by mixing 0.1 g of adsorbent with 50 mL of 10 ppm MB. The mixture was agitated at room temperature (RT) in a shaking water bath for 4 h then centrifuged at 8,000 rpm for 30 min to separate the adsorbent of the liquid phase. The dye concentration before and after the adsorption determined. A schematic diagram of the adsorption process presented in Fig. 2.

Dye removal percentage was calculated according to the following formula [24]:

$$\text{Dye removal (\%)} = \left[ \frac{(C_0 - C_t)}{C_0} \right] \times 100 \quad (1)$$

where  $C_0$  and  $C_t$  ( $\text{mg L}^{-1}$ ), are the initial at zero time and the final concentration of MB at a definite time, respectively.

The removal capacity calculated according to the following formula [24]:

$$q (\text{mg g}^{-1}) = \frac{V(C_0 - C_t)}{M} \quad (2)$$

where  $q$  is the uptake capacity ( $\text{mg g}^{-1}$ );  $V$  is the volume of the MB solution (mL), and  $M$  is the mass of the PAN or HPAN (g).

## 3. Results and discussions

### 3.1. Effect of MB concentration

Varied of the MB concentrations affected the adsorption capacity of the PAN and HPAN nanoparticles, as shown in Fig. 3. It can seem that increasing the MB concentration up to 7 ppm increased the adsorption capacity linearly. Further

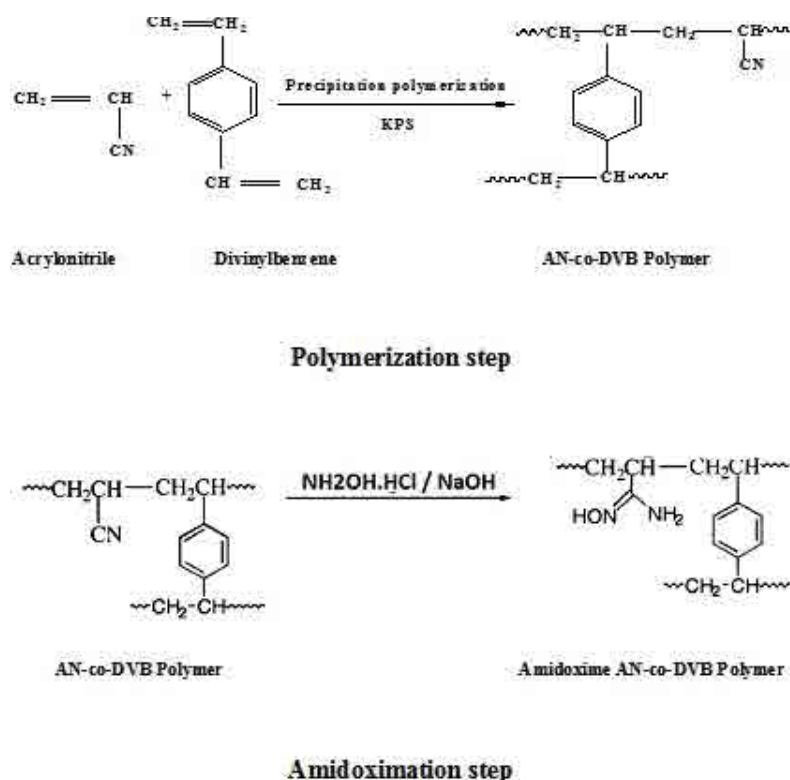


Fig. 1. Proposed polymerization and amidoximation reactions.

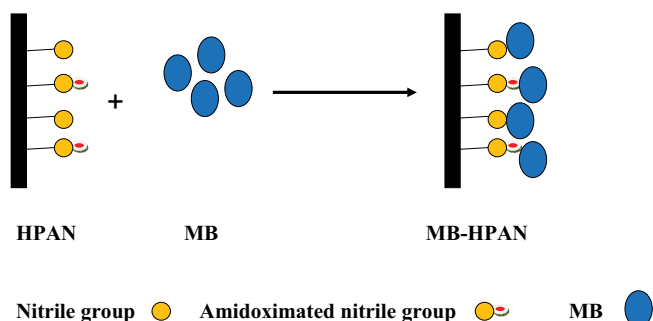


Fig. 2. MB adsorption by HPAN nanoparticles.

increase of the MB concentration up to 15 ppm, the adsorption capacity started to show a lower rate of increment. Such behavior is an indication of the closeness reach to the saturation of the adsorption centers over the polymer matrices surfaces. The HPAN nanoparticles show higher adsorption capacity than the PAN counterpart only at higher MB concentrations. Both adsorbents show the maximum capacity at 15 ppm, 2.25 mg g<sup>-1</sup>, and 1.95 mg g<sup>-1</sup> for HPAN and PAN. Our results are following other published results [28–30].

### 3.2. Adsorption isotherm models

Adsorption isotherms are mathematical models that describe the distribution of the adsorbate species among solid and liquid phases and are thus crucial from the chemical design point of view. The results obtained on the adsorption

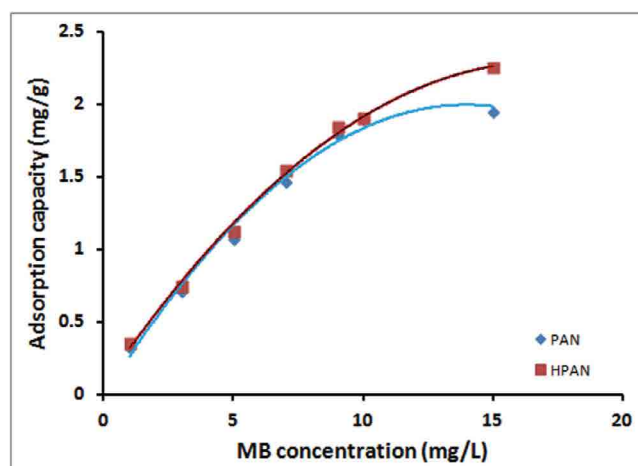


Fig. 3. Effect of the MB concentrations on the adsorption capacity of the PAN and HPAN nanoparticles.

of MB onto the synthesized PAN and HPAN analyzed by the well-known models given by Freundlich, Langmuir, Temkin, and Harkins-Jura. The sorption data obtained for equilibrium conditions have analyzed by using the linear forms of these kinds of isotherms.

The Freundlich isotherm is a widely used equilibrium isotherm model but provides no information on the monolayer sorption capacity, in contrast to the Langmuir model [31,32]. The Freundlich isotherm model assumes neither homogeneous site energies nor limited levels of sorption.

The Freundlich model is the earliest known empirical equation and is shown to be consistent with an exponential distribution of active centers, characteristic of heterogeneous surfaces [33].

$$\ln q_e = \ln K_F + \frac{1}{n_f} \ln C_e \quad (3)$$

where  $K_F$  is the Freundlich constant depicts adsorption capacity, and  $n_f$  is a constant indicating adsorption intensity. With plotting  $\ln q_e$  against  $\ln C_e$ , a straight line with slope  $1/n_f$  and intercept  $\ln K_F$  obtained. The intercept of the line,  $K_F$ , indicates roughly of the adsorption capacity with slope,  $n_f$ , as an indicator of adsorption effectiveness. For the adsorption isotherms, initial MB concentration was varied while the pH and temperature of the solution, the agitation speed and adsorbent weight in each sample were held constant.

Linear fits of sorption data of the MB given in Fig. 4a. According to the correlation coefficient ( $R^2$ ) values, 0.9671 and 0.9856 for PAN and HPAN, it was demonstrated that the removal of MB using HPAN polymer obeyed the Freundlich isotherm better than the PAN polymer. The values of Freundlich constants  $n_f$  and  $K_F$  that estimated from the slope

and intercept of the linear plot were 1.77 and 0.61 for PAN and 1.8 and 0.66 for HPAN. From the estimated value of  $n_f$  it found that  $n_f > 1$  indicating favorable adsorption for MB using both synthesized PAN and HPAN nanoparticles [34]. The adsorption capacity of the HPAN is double that of the PAN counterpart.

The Langmuir equation, which is valid for monolayer sorption onto a completely homogeneous surface with a finite number of identical sites and with negligible interaction between adsorbed molecules, is given by the following equation [35]:

$$\frac{C_e}{q_e} = \frac{1}{q_m K} + \frac{C_e}{q_m} \quad (4)$$

where  $q_e$  is the amount of adsorbed ( $\text{mg g}^{-1}$ ).  $C_e$  is the equilibrium concentration of the adsorbate ions ( $\text{mg L}^{-1}$ ).  $q_m$  and  $K$  are Langmuir constants related to maximum adsorption capacity (monolayer capacity) ( $\text{mg g}^{-1}$ ) and energy of adsorption ( $\text{L mg}^{-1}$ ).

Plotting of  $C_e/q_e$  vs.  $C_e$  indicates a straight line with  $1/q_m$  slope and an intercept of  $1/q_m K$ . Fig. 4b illustrates the linear plot of the Langmuir equation for the MB removal using the

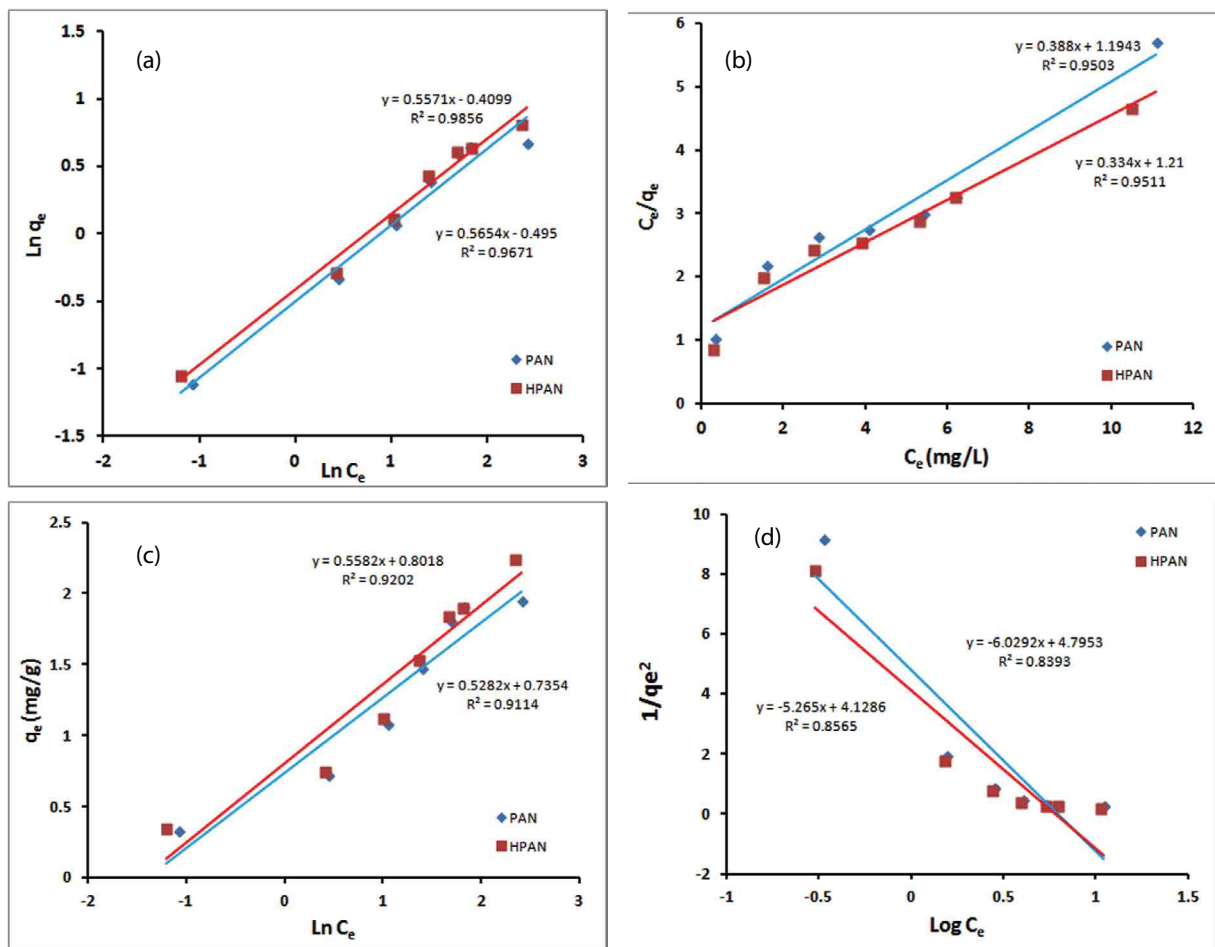


Fig. 4. (a) Freundlich, (b) Langmuir, (c) Temkin, and (d) Harkin-Jura isotherm for the MB removal using the PAN and HPAN nano-particles with various MB initial solution concentrations.

synthesized polymers at various initial MB concentrations. The value of the correlation coefficient ( $R^2$ ) is considered an indicator of the goodness-of-fit of experimental data on the isotherm's model. The  $R^2$  values were 0.9503 and 0.9511 for PAN and HPAN polymers indicating a good mathematical fit of the adsorption data using both adsorbents; HPAN and PAN polymers.

Langmuir parameters for MB removal,  $q_m$ , and  $K$ , were calculated from the slope and intercept of Fig. 4b. It found from the computed value of  $q_m$  that equal 2.58 and 3.0 mg g<sup>-1</sup> for PAN and HPAN. These results indicate that the HPAN polymer has higher efficiency and energy of adsorption for the MB removal than that of the PAN polymer; 3.078 and 3.620 L mg<sup>-1</sup> for PAN and HPAN.

The dimensionless separation factor, which considers as essential characteristics of the Langmuir isotherms, is calculated.  $R_L$  predict whether an adsorption system is favorable or unfavorable and defined as [36]:

$$R_L = \frac{1}{1 + KC_0} \quad (5)$$

Values of  $R_L$  (Table 1) for the MB removal fall between zero and one show favorable adsorption [37]. That confirmed the adsorption of the MB onto the synthesized polymers under the conditions used in this study was favorable by Langmuir isotherm.

Temkin isotherm considered the effects of indirect adsorbent/adsorbate interactions on the adsorption process. The heat of adsorption of all the molecules in the layer would decrease linearly with coverage due to adsorbent/adsorbate interactions [38]. It can express in the linear form as [39,40]:

$$q_e = B \ln K_T + B \ln C_e \quad (6)$$

A plot of  $q_e$  vs.  $\ln C_e$  (Fig. 4c) enables the determination of the isotherm constants  $B$  and  $K_T$  from the slope and the intercept. From Fig. 4, the calculated  $K_T$  equal to 4.0 and 4.2 L g<sup>-1</sup>, which represents the equilibrium binding constant corresponding to the maximum binding energy. The constant  $B$  that equal to 0.5582 and 0.5282 J mol<sup>-1</sup> is related to the heat of adsorption for PAN and HPAN, respectively.

Finally, the Harkins-Jura adsorption isotherm can be expressed as [41,42].

$$\frac{1}{q_e^2} = \left( \frac{B_H}{A_H} \right) - \left( \frac{1}{A_H} \right) \log C_e \quad (7)$$

The Harkins-Jura adsorption isotherm accounts for multilayer adsorption and can be explained with the existence of heterogeneous pore distribution. The value of  $1/q_e^2$  plotted against  $\log C_e$ . Where  $B_H$  (intercept/slope; mg<sup>2</sup> L<sup>-1</sup>) and  $A_H$  (1/slope; g<sup>2</sup> L<sup>-1</sup>) are the isotherm constants; Fig. 4d.

The Harkins-Jura isotherm is analogous to the Freundlich model in addition to considering the existence of a heterogeneous pores distribution. The model shows the lowest fit of the results where  $R^2$  values; 0.8393 and 0.8565 for the PAN and HPAN polymers. The obtained results indicate the formation of multilayers of adsorption and the existence of a homogeneous pores distribution in both adsorbents.

All the isotherm parameters including the correlation coefficient,  $R^2$  values and adsorption capacity at equilibrium (maximum adsorption capacity) obtained from the four equilibrium isotherm models applied for the MB adsorption on the synthesized polymers summarized in Table 2. The Freundlich isotherm model gave the highest  $R^2$  value for both adsorbents, PAN (0.9671) and HPAN (0.9856), showing that this model best described the MB sorption on the synthesized polymers. That suggested the formation of multilayers of adsorption [41,42].

### 3.3. Effect of adsorption time

The result of varying the adsorption time over 7 h on the removal of the MB dye from synthetic solution (10 ppm) using 0.1 g adsorbent at RT followed; Fig. 5. From Fig. 5, we can see that a linear increment removal of the MB has observed over the first 3 h. After mentioned, a lower rate of removal has been detected to reach almost equilibrium after 7 h. Generally, the HPAN has a faster rate of removal than PAN referred to the posses of additional exchangeable sites resulted from the hydroximation process [24]. Other authors have observed a similar trend used modified PAN with monoethanolamine [29] and iminated PAN [30]. The adsorption capacities of both adsorbents detected at equilibrium are close despite the functionalization of the HPAN with other adsorption sites; 2.1 and 2.35 mg g<sup>-1</sup> for PAN and HPAN nanoparticles.

### 3.4. Adsorption kinetic models

Adsorption is a physiochemical process involves the mass transfer of a solute from the liquid phase to the adsorbent surface.

A study of the kinetics of adsorption is desirable as it provides information about the mechanism of adsorption, which is essential for an efficient process.

The most common models used to fit the kinetic sorption experiments are Lagergren's pseudo-first-order model (Eq. (8)) [38], pseudo-second-order model (Eq. (9)) [39], and Elovich model (Eq. (10)) [43].

$$\ln(q_e - q_t) = \ln q_e - k_1 t \quad (8)$$

Table 1  
The  $R_L$  values of PAN and HPAN adsorbents

| $C_0$ | $R_L$ PAN | $R_L$ HPAN |
|-------|-----------|------------|
| 1     | 0.245     | 0.217      |
| 3     | 0.098     | 0.084      |
| 5     | 0.061     | 0.052      |
| 7     | 0.044     | 0.038      |
| 9     | 0.035     | 0.030      |
| 10    | 0.032     | 0.027      |
| 15    | 0.021     | 0.018      |

Table 2

Parameters and the correlation coefficients of the Langmuir, the Freundlich, the Temkin and the Harkin-Jura (H-J) isotherm models

| Adsorbent | Langmuir isotherm                   |                                |        | Freundlich isotherm            |       |        | Temkin isotherm                 |                               |        | Harkin-Jura (H-J) |                                |        |        |
|-----------|-------------------------------------|--------------------------------|--------|--------------------------------|-------|--------|---------------------------------|-------------------------------|--------|-------------------|--------------------------------|--------|--------|
|           | $q_{\max}$<br>(mg g <sup>-1</sup> ) | $K_L$<br>(L mg <sup>-1</sup> ) | $R^2$  | $K_F$<br>(mg g <sup>-1</sup> ) | $n_f$ | $R^2$  | $B_t$<br>(J mol <sup>-1</sup> ) | $K_T$<br>(L g <sup>-1</sup> ) | $R^2$  | $A_H$             | $V_m$<br>(mg g <sup>-1</sup> ) | $B_H$  | $R^2$  |
| PAN       | 2.58                                | 3.078                          | 0.9503 | 0.61                           | 1.77  | 0.9671 | 0.5582                          | 4.0                           | 0.9114 | -2.85             | 0.1659                         | 0.7953 | 0.8393 |
| HPAN      | 3.00                                | 3.620                          | 0.9511 | 0.66                           | 1.80  | 0.9856 | 0.5282                          | 4.2                           | 0.9204 | -5.16             | 0.1899                         | 0.7841 | 0.8565 |

$$\frac{t}{q_t} = \frac{1}{k_2 q_e^2} + \frac{t}{q_e} \quad (9)$$

$$q_t = \alpha + \beta \ln t \quad (10)$$

where  $q_e$  (mg g<sup>-1</sup>) and  $q_t$  (mg g<sup>-1</sup>) are the amount of dye adsorbed at equilibrium and at time  $t$ , respectively.  $k_1$  (min<sup>-1</sup>) and  $k_2$  (g mg<sup>-1</sup> min) are the pseudo-first-order and pseudo-second-order adsorption rate constants, respectively. The Elovich constants are  $\alpha$  (mg g<sup>-1</sup> min<sup>-1</sup>), the initial sorption rate, and  $\beta$  (g mg<sup>-1</sup>), the extent of surface coverage and activation energy for chemisorption.

#### 3.4.1. Pseudo-first-order model

The pseudo-first-order kinetic model was the earliest model about the adsorption rate based on the adsorption capacity. The values of the pseudo-first-order constant ( $k_1$ ; 0.558 and 0.597 for PAN and HPAN) and correlation coefficient ( $R^2$ ; 0.9875 and 0.9703 for PAN and HPAN) obtained from the slope of the plot  $\ln(q_e - q_t)$  vs. time in Fig. 6a. It indicated that the correlation coefficients are good enough. However, the estimated values of  $q_e$  calculated from the equation; 1.546 and 2.03 mg g<sup>-1</sup>, have differed from the experimental values, 2.1 and 2.35 mg g<sup>-1</sup>, for PAN and HPAN (Table 3).

#### 3.4.2. Pseudo-second-order model

The experimental kinetic data were further analyzed using the pseudo-second-order model. By plotting  $t/q_t$  against  $t$  for MB, a straight line obtained in all cases. And using the second-order rate constant ( $k_2$ ; 0.3976 and 0.3979 for PAN and HPAN) and  $q_e$  values (2.37 and 2.70 for PAN and HPAN) determined from the slope and intercept of the plot, Fig. 6b. The values of the correlation coefficients,  $R^2$  for the adsorption of MB on PAN and HPAN were found almost equal to one (Table 3). Accordingly, the kinetics of MB adsorption on to PAN and HPAN can be described well by the second-order equation in agreement with other published results [29,30]. That suggests the rate-limiting step in these sorption processes may be chemisorption. The valent forces through the sharing or exchange of electrons between adsorbent and adsorbate involved [44].

#### 3.4.3. Elovich model

The simple Elovich model is one of the most useful models for describing the kinetics of chemisorption of gas onto

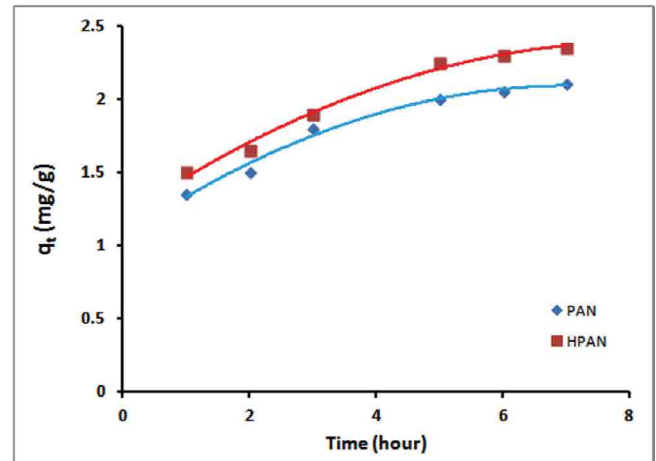


Fig. 5. Effect of the adsorption time on the adsorption capacity of the PAN and HPAN nanoparticles.

solid systems. However, recently, it has also been applied to describe the adsorption process of pollutants from aqueous solutions. Fig. 6c illustrates the plot of  $q_t$  against  $\ln t$  for the sorption of MB onto PAN and HPAN. From the slope and intercept of the linearization of the simple Elovich equation, the estimated Elovich equation parameters obtained (Table 3). The values of  $\beta$  indicate the number of sites available for adsorption (0.4107 and 0.4761 for PAN and HPAN). The  $\alpha$  values indicate the adsorption quantity when  $\ln t$  is equal to zero; that is, the adsorption quantity when  $t$  is 1 h (1.3106 and 1.4244 for PAN and HPAN). This value helps understand the adsorption behavior of the first step [45]. Also, from this Fig., it was declared that the Elovich equation fits well with the experimental data.

#### 3.5. Sorption mechanism models

Following up the adsorption mechanism of any ions onto solid from aqueous phase is going through a multi-step process. Initially, two steps recognized in the liquid phase. The first step is the transport of the ions from the aqueous phase to the surface of the solid particles, which is known as bulk diffusion. This step followed by diffusion of the ions via the boundary layer to the surface of the solid particles (film diffusion). The last step is, consequently, happened in the solid phase where the ions transport from the solid particles surfaces to its interior pores, known as pore diffusion or intraparticle diffusion. This step is likely to be slow, and therefore, it may be considered as the rate-determining step.

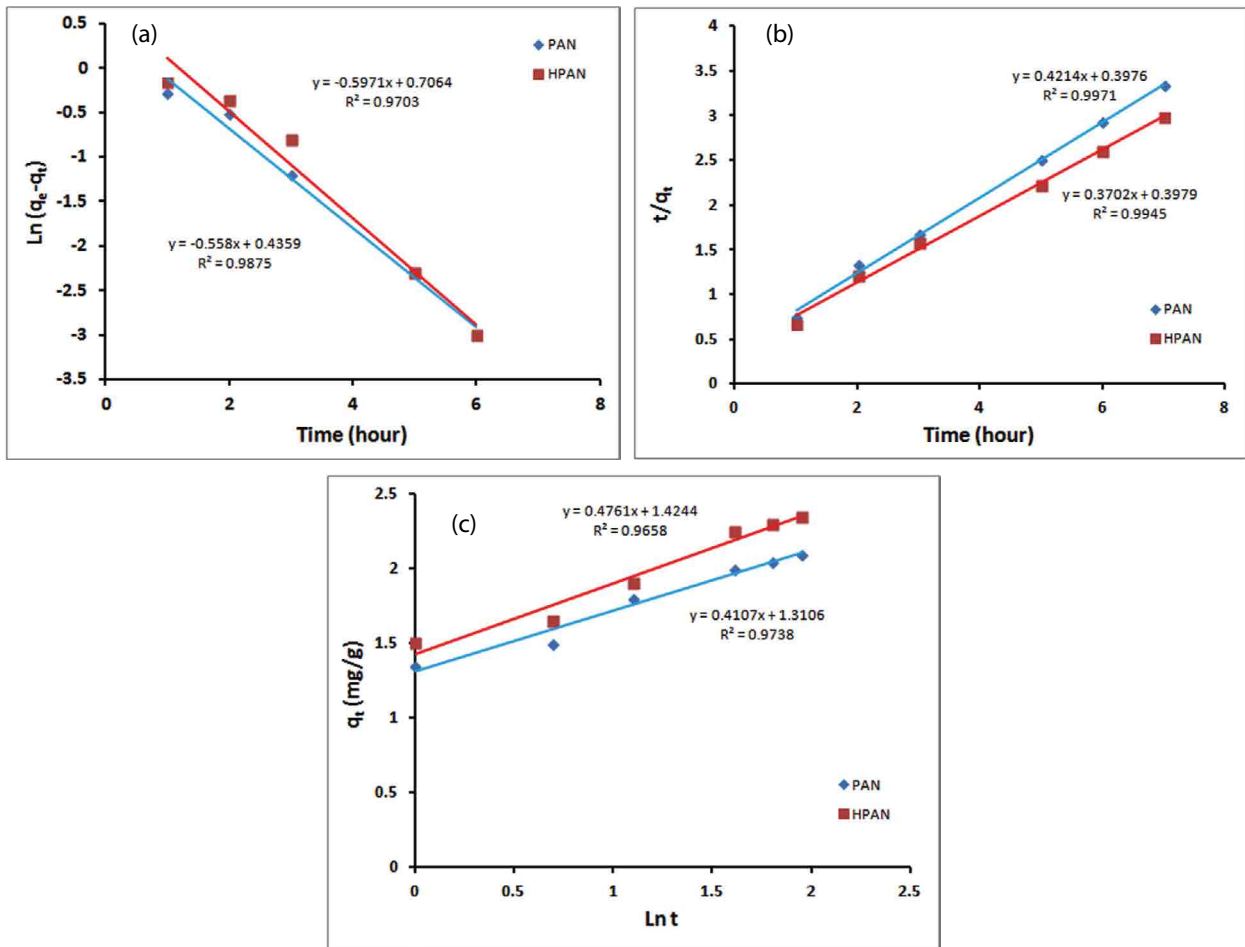


Fig. 6. (a) First-order (b) Second-order, and (c) Simple Elovich plots for the MB removal using the PAN and HPAN nanoparticles.

Table 3  
Adsorption parameters of the pseudo-second, the pseudo-first-order, and the Elovich kinetic models

| Adsorbent | Pseudo-second-order                   |                                       |   |        | Pseudo-first-order                    |                               |        | Elovich                          |   |        |
|-----------|---------------------------------------|---------------------------------------|---|--------|---------------------------------------|-------------------------------|--------|----------------------------------|---|--------|
|           | $q_{e,exp.}$<br>(mg g <sup>-1</sup> ) | $q_{e,cal.}$<br>(mg g <sup>-1</sup> ) | $k_2$<br>(m <sup>2</sup> mg <sup>-1</sup> min <sup>-1</sup> ) | $R^2$  | $q_{e,cal.}$<br>(mg g <sup>-1</sup> ) | $k_1$<br>(min <sup>-1</sup> ) | $R^2$  | $\beta$<br>(g mg <sup>-1</sup> ) | $\alpha$<br>(mg g <sup>-1</sup> min <sup>-1</sup> ) | $R^2$  |
| PAN       | 2.1                                   | 2.37                                  | 0.3976  | 0.9971 | 1.546                                 | -0.588                        | 0.9875 | 0.4107                           | 1.3106  | 0.9738 |
| HPAN      | 2.35                                  | 2.70                                  | 0.3979  | 0.9945 | 2.03                                  | -0.597                        | 0.9703 | 0.4761                           | 1.4244  | 0.9658 |

Adsorption of an ion at an active site on the solid phase surface could also occur through a chemical reaction such as ion-exchange, complexation, and chelation.

The diffusion rate equations inside particulate of Dumwald-Wagner and intraparticle models were used to calculate the diffusion rate of MB on polymers particles. On the other hand, concerning the external mass transfer, Boyd [53] model was examined to determine the actual rate-controlling step for MB removal.

Usually, the sorption process controlled by either the intraparticle (pore diffusion) or the liquid-phase mass transport rates (film diffusion) [46]. Experimenting is a batch system with rapid stirring leaves the possibility that intraparticle diffusion is the rate-determining step [47]. Weber and

Morris [48] explored the possibility of affecting the adsorption process via intra-particle diffusion resistance using the intra-particle diffusion model described as follows:

$$q_t = k_{id}t^{1/2} + I \tag{11}$$

where  $k_{id}$  is the intra-particle diffusion rate constant. Kannan et al. [49] have figured out the thickness of the boundary layer from the values of the  $I$ . Greater boundary layer effect noticed with a larger intercept. The plot of  $q_t$  vs.  $t^{0.5}$  was presented in Fig. 7a using PAN and HPAN. Two separate linear portions that represent each line could observe from the figure. That suggests the removal process consists of both

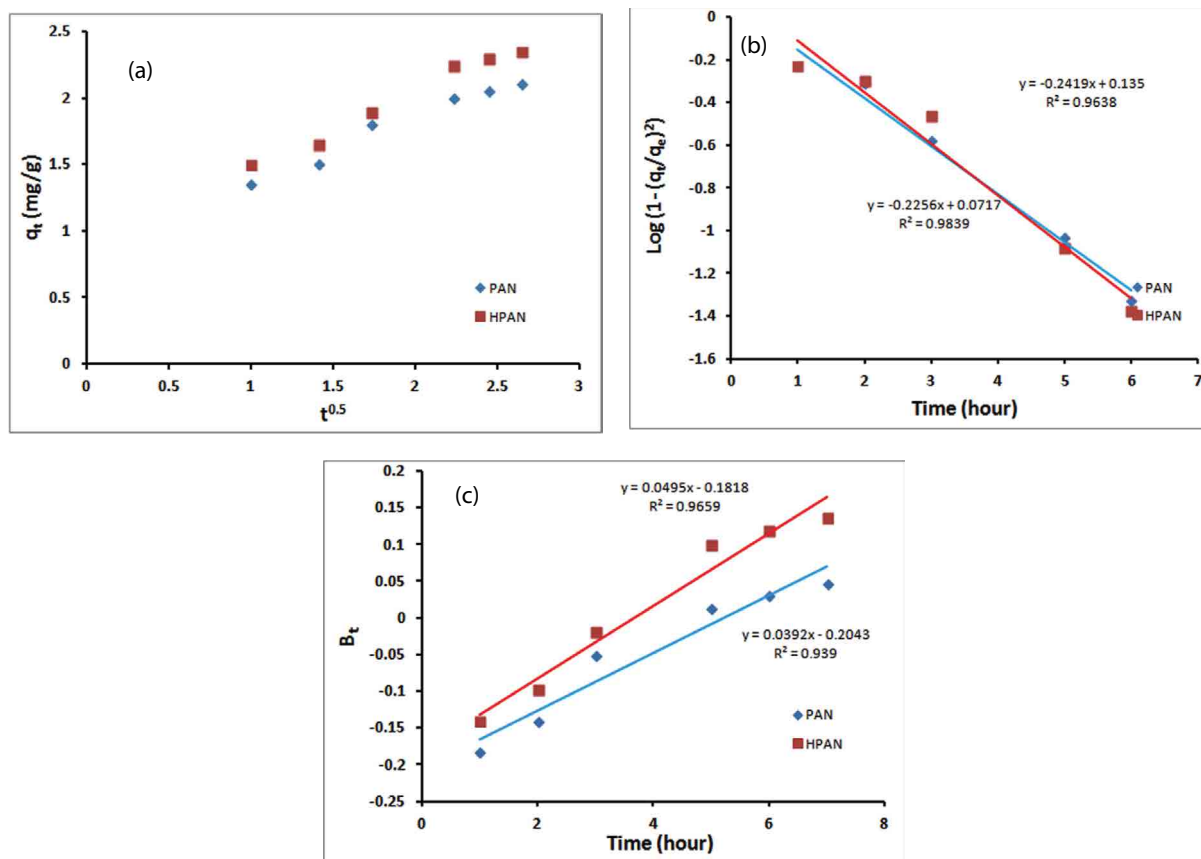


Fig. 7. (a) Intraparticle diffusion plots, (b) Dumwald–Wagner plots, and (c) Boyd expression for the removal of the MB using the PAN and HPAN nanoparticles.

surface removal and intraparticle diffusion. While the initial linear part of the plot is the indicator of the existence of the boundary layer effect, the second linear portion is due to intraparticle diffusion [50]. The intraparticle diffusion rate ( $k_d$ ), 0.2415 and 0.2415 ( $\text{mg g}^{-1} \text{min}^{-1}$ ) for PAN and HPAN, calculated from the slope of the second linear portion and the values of  $C$  (1.4596 and 1.7096), the intercept, provides an idea about the thickness of the boundary layer. The larger the intercept, the greater is the boundary layer effect [49].

In case of involving the intraparticle diffusion in the sorption process, then a linear relationship would result from the plot of  $q_t$  vs.  $t^{1/2}$ . The intraparticle diffusion would be the controlling step if this line passed through the origin [46]. Fig. 7a confirms straight lines not passed through the origin. The difference between the rate of mass transfer in the initial and final steps of the sorption process may cause the deviation of straight lines from the origin. Accordingly, it can conclude that the pore diffusion is not the sole rate-controlling step [51]. Additional processes, such as the adsorption on the boundary layer, may also be involved in the control of the adsorption rate.

The diffusion rate equation inside particulate of Dumwald–Wagner can be expressed as [52]:

$$\log(1-F^2) = -\left(\frac{K}{2.303}\right) \times t \quad (12)$$

where  $K$  is the diffusion rate constant and the removal percent,  $F$  is calculated by  $(q_t/q_e)$ . The proper linear plot of  $\log(1-F^2)$  vs.  $t$  (Fig. 7b) indicates the applicability of this kinetic model. The diffusion rate constants  $K$  for MB diffusion inside PAN and HPAN particles found  $-0.5196$  and  $-0.5571 \text{ min}^{-1}$ .

The kinetic expression further analyzed the adsorption data is given by Boyd et al. [53] to characterize what the actual rate-controlling step involved in the MB sorption process.

$$F = 1 - \left(\frac{6}{\pi^2}\right) \exp(-B_t) \quad (13)$$

where  $F$  is the fraction of solute sorbed at different time  $t$  and  $B_t$  is a mathematical function of  $F$  and given by the following equation:

$$F = \frac{q}{q_e} \quad (14)$$

where  $q$  and  $q_e$  represent the amount sorbed ( $\text{mg g}^{-1}$ ) at any time  $t$  and at the infinite time (in the present study 7 h). With substituting Eq. (13) into Eq. (14), the kinetic expression becomes:

$$B_t = -0.4978 - \ln\left(1 - \frac{q}{q_e}\right) \quad (15)$$

Thus, the value of  $B_t$  can calculate for each value of “ $F$ ” using Eq. (15). The calculated  $B_t$  values were plotted against time, as shown in Fig. 7c. The linearity of this plot will provide useful information to distinguish between external transport- and intraparticle-transport controlled rates of sorption. Fig. 7c shows the plot of  $B_t$  vs.  $t$ , which is a straight line that does not pass through the origin, indicating that film diffusion governs the rate-limiting process [54].

### 3.6. Adsorption thermodynamic studies

The effect of variation adsorption temperature illustrated in Fig. 8. A negative impact of elevating the adsorption temperature of MB has observed on both adsorbents. Such finding is an indication of the exothermic nature of the MB adsorption process on both adsorbents. The exothermic nature of the MB adsorption is evident in the case of PAN adsorbent.

The thermodynamic parameters should be taken into consideration to conclude the spontaneity of the adsorption process. A spontaneous system will display a decrease in  $\Delta G^\circ$  and  $\Delta H^\circ$  values with increasing the temperature. All the thermodynamic parameters calculated from the following equations [55,56]:

$$\ln K_0 = \frac{\Delta S}{R} - \frac{\Delta H}{RT} \tag{16}$$

where:

$$K_0 = \frac{q_e}{C_e} \tag{17}$$

$$\Delta G = -RT \ln K_0 \tag{18}$$

where  $R$  is the gas constant ( $8.314 \text{ J mol}^{-1} \text{ K}^{-1}$ ), and  $T$  is the temperature in K. Table 4 lists down the values for the thermodynamic parameters (Fig. 9). The negative value for the  $\Delta H^\circ$  ( $13.468$  and  $7.898 \text{ kJ mol}^{-1}$ ) for PAN and HPAN adsorbents indicates the exothermic nature of the process. That explains the decrease of MB adsorption efficiency as the temperature increased. According to Alkan et al. [57], the enthalpy change values resulted from the chemisorption are between  $40$  and  $120 \text{ kJ mol}^{-1}$ . That values are larger than that caused by the physisorption. Consequently, the lower value of the heat of adsorption acquired in this study indicates that the adsorption of metal ions is probably attributable to the physisorption.

Conversely, in the kinetics study, it was described that the adsorption is chemisorption. The lower  $\Delta H^\circ$  value indicated that the physisorption also takes part in the adsorption process. The MB ions adhere to the adsorbent surface only through weak intermolecular interactions. The positive value

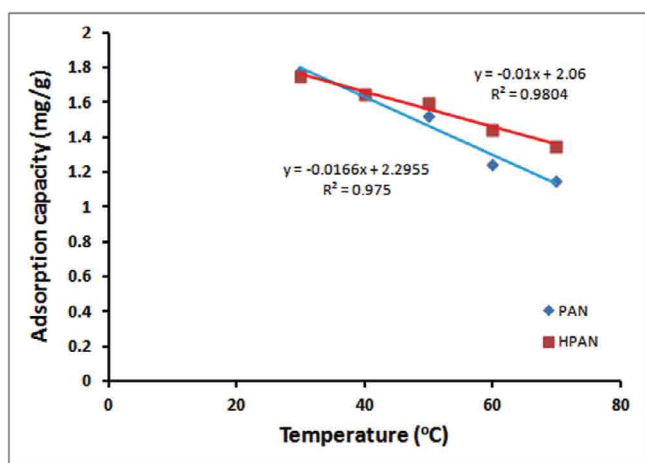


Fig. 8. Effect of the adsorption temperature on the adsorption capacity of the PAN and HPAN nanoparticles.

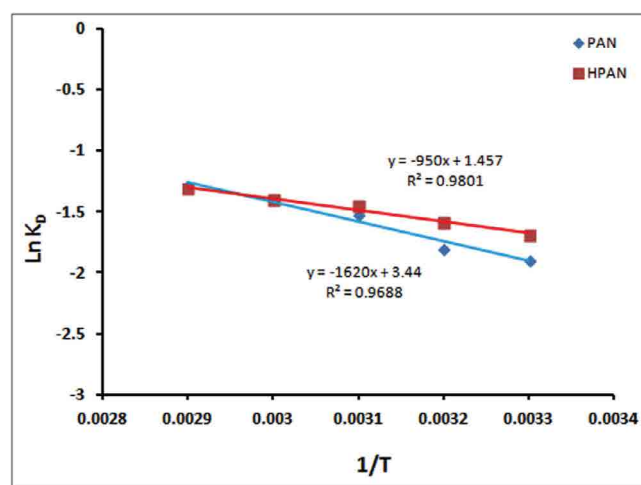


Fig. 9. Van't Hoff plot of the adsorption of MB removal using the PAN and HPAN nanoparticles.

Table 4  
Thermodynamic parameters

| Temperature (°C) | PAN                                |                                    |   | HPAN                               |                                    |   |
|------------------|------------------------------------|------------------------------------|---|------------------------------------|------------------------------------|---|
|                  | $\Delta G$ (kJ mol <sup>-1</sup> ) | $\Delta H$ (kJ mol <sup>-1</sup> ) | $\Delta S$ (J K <sup>-1</sup> mol <sup>-1</sup> ) | $\Delta G$ (kJ mol <sup>-1</sup> ) | $\Delta H$ (kJ mol <sup>-1</sup> ) | $\Delta S$ (J K <sup>-1</sup> mol <sup>-1</sup> ) |
| 30               | 3.249                              | -13.468                            | 28.6  | 3.3                                | -7.898                             | 12.11   |
| 40               | 3.643                              |                                    |   | 3.643                              |                                    |   |
| 50               | 4.081                              |                                    |   | 3.894                              |                                    |   |
| 60               | 4.983                              |                                    |   | 4.402                              |                                    |   |
| 70               | 5.418                              |                                    |   | 4.819                              |                                    |   |

for the entropy change,  $\Delta S^\circ$  (28.6 and 12.11 J mol<sup>-1</sup> K<sup>-1</sup>) for PAN and HPAN adsorbents are illustrating the disorderliness at the solid/liquid interface during the adsorption of MB ions where the  $\Delta G^\circ$  values reflect the feasibility of the process.

#### 4. Conclusion

PAN-based adsorbents developed for the removal of MB from a synthetic solution successively prepared. The impact of varying the MB concentration on the adsorption capacity was found a positive one with increasing of the MB concentration up to 7 ppm. Further increase of the MB concentration has no significant impact on the adsorption capacity. A linear positive effect of the adsorption time observed up to 5 h where adsorption equilibrium almost reached. The adsorption capacity obtained at the lowest temperature was the maximum indicating the exothermic nature of the adsorption process. The kinetics of the adsorption process was found to follow the pseudo-second-order kinetic model and the inter-particulate diffusion model suggests that the pore diffusion is not the sole rate-controlling step. Moreover, the applicability of the Boyd [53] model indicates that the film diffusion governs the rate-limiting process. The adsorption process isotherm of the MB molecules observed as multilayer one which followed the Freundlich isotherm model. The maximum monolayer adsorption capacity determined according to the Langmuir isotherm model for MB removal,  $q_m$ , equal to 2.58 and 3.0 mg g<sup>-1</sup> for PAN and HPAN.

#### References

- [1] S. Haider, Y. Khan, W. Al-masry, A. Haider, Z. Ullah, R. Ullah, *Electrospun Nanofibers and Their Functionalization*, Nova Publishers Inc., New York, NY, 2013, pp. 75–92.
- [2] K. Saeed, S. Haider, T.-J. Oh, S.-Y. Park, Preparation of amidoxime-modified polyacrylonitrile (PAN-oxime) nanofibers and their applications to metal ions adsorption, *J. Membr. Sci.*, 322 (2008) 400–405.
- [3] Ratna, B.S. Padhi, Pollution due to synthetic dyes toxicity & carcinogenicity studies and remediation, *Int. J. Environ. Sci.*, 3 (2012) 940–955.
- [4] Q.Y. Sun, L.Z. Yang, The adsorption of basic dyes from aqueous solution on modified peat-resin particle, *Water Res.*, 37 (2003) 1535–1544.
- [5] M.N.V. Ravi Kumar, T.R. Sridhari, K.D. Bhavani, P.K. Dutta, Trends in color removal from textile mill effluents, *Colorage*, 40 (1998) 25–34.
- [6] M.M. Abd El-Latif, A.M. Ibrahim, Adsorption, kinetic and equilibrium studies on removal of basic dye from aqueous solutions using hydrolyzed Oak sawdust, *Desal. Wat. Treat.*, 6 (2009) 252–268.
- [7] M. Leszczyńska, Z. Hubicki, Application of weakly and strongly basic anion exchangers for the removal of brilliant yellow from aqueous solutions, *Desal. Wat. Treat.*, 2 (2009) 156–161.
- [8] A.E. Ofomaja, Equilibrium sorption of methylene blue using mansonia wood sawdust as biosorbent, *Desal. Wat. Treat.*, 3 (2009) 1–10.
- [9] S. Haider, N. Bukhari, S.Y. Park, Y. Iqbal, W.A. Al-Masry, Adsorption of bromo-phenol blue from an aqueous solution onto thermally modified granular charcoal, *Chem. Eng. Res. Des.*, 89 (2011) 23–28.
- [10] R. Sanghi, P. Verma, Decolorisation of aqueous dye solutions by low-cost adsorbents: a review, *Color. Technol.*, 118 (2002) 256–269.
- [11] J.P. Chen, L. Hong, S. Wu, L. Wang, Elucidation of interactions between metal ions and Ca alginate-based ion-exchange resin by spectroscopic analysis and modeling simulation, *Langmuir*, 18 (2002) 9413–9421.
- [12] L. Jin, R. Bai, Mechanisms of lead adsorption on chitosan/PVA hydrogel beads, *Langmuir*, 18 (2002) 9765–9770.
- [13] R. Coşkun, M. Yiğitoğlu, M. Saçak, Adsorption behavior of copper(II) ion from aqueous solution on methacrylic acid-grafted poly(ethylene terephthalate) fibers, *J. Appl. Polym. Sci.*, 75 (2000) 766–772.
- [14] S. Lacour, J.-C. Bollinger, B. Serpaud, P. Chantron, R. Arcos, Removal of heavy metals in industrial wastewaters by ion-exchanger grafted textiles, *Anal. Chim. Acta*, 428 (2001) 121–132.
- [15] C.A. Borgo, Y. Gushikem, Zirconium phosphate dispersed on a cellulose fiber surface: preparation, characterization, and selective adsorption of Li<sup>+</sup>, Na<sup>+</sup>, and K<sup>+</sup> from aqueous solution, *J. Colloid Interface Sci.*, 246 (2002) 343–347.
- [16] R.X. Liu, Y. Li, H.X. Tang, Synthesis and characteristics of chelating fibers containing imidazoline group or thioamide group, *J. Appl. Polym. Sci.*, 83 (2002) 1608–1616.
- [17] T.M.A. Hossain, H. Maeda, T. Iijima, Z. Morita, Diffusion of cationic dye into polyacrylonitrile, *J. Polym. Sci., Part C: Polym. Lett.*, 5 (1967) 1069–1072.
- [18] D. Şuteu, D. Bîlbă, C. Zaharia, HPAN textile fiber wastes for removal of dyes from industrial textile effluent, *Bull. Transilvania Univ. Braşov*, 2 (2009) 218–223.
- [19] L. Boguslavsky, S. Baruch, S. Margel, Synthesis and characterization of polyacrylonitrile nanoparticles by dispersion/emulsion polymerization process, *J. Colloid Interface Sci.*, 289 (2005) 71–85.
- [20] T. Biswal, P.K. Sahoo, Synthesis of PAN nanoparticles via nonconventional microemulsion technique using Co(II)/EDTA in situ complex, *Indian J. Chem. Technol.*, 14 (2007) 119–125.
- [21] J.-M. Lee, S.-J. Kang, S.-J. Park, Synthesis of polyacrylonitrile based nanoparticles via aqueous dispersion polymerization, *Macromol. Res.*, 17 (2009) 817–820.
- [22] T. Biswal, R. Samal, P.K. Sahoo, Complex-mediated microwave-assisted synthesis of polyacrylonitrile nanoparticles, *Nanotechnol. Sci. Appl.*, 3 (2010) 77–83.
- [23] F. Sebesta, J. John, A. Motl, K. Stamberg, Evaluation of Polyacrylonitrile (PAN) as a Binding Polymer for Absorbents Used to Treat Liquid Radioactive Wastes, Other Information: PBD: Nov 1995, ed., US Government Printing Office Department, United States, 1995, 50 p.
- [24] M.S. Mohy Eldin, S.A. El-Sakka, M.M. El-Masry, I.I. Abdel-Gawad, S.S. Garybe, Removal of methylene blue dye from aqueous medium by nano poly acrylonitrile particles, *Desal. Wat. Treat.*, 44 (2012) 151–160.
- [25] M.S. Mohy Eldin, Y.A. Aggour, M.R. El-Aassar, G.E. Beghet, R.R. Atta, Development of nano-crosslinked polyacrylonitrile ions exchanger particles for dyes removal, *Desal. Wat. Treat.*, 57 (2016) 4255–4266.
- [26] M.S. Mohy Eldin, M.H. Gouda, M.A. Abu-Saied, Y.M.S. El-Shazly, H.A. Farag, Development of grafted cotton fabrics ions exchanger for dye removal applications: methylene blue model, *Desal. Wat. Treat.*, 57 (2016) 22049–22060.
- [27] M.S. Mohy Eldin, M.H. Gouda, M.E. Youssef, Y.M.S. El-Shazly, H.A. Farag, Removal of methylene blue by amidoxime polyacrylonitrile-grafted cotton fabrics: kinetic, equilibrium, and simulation studies, *Fibers Polym.*, 17 (2016) 1884–1897.
- [28] A. Salisu, M.M. Sanagi, A. Abu Naim, K.J. Karim, Removal of methylene blue dye from aqueous solution using alginate grafted polyacrylonitrile beads, *Der Pharma Chemica*, 7 (2015) 237–242.
- [29] G. Kiani, M. Khodagholizadeh, M. Soltanzadeh, Removal of methylene blue by modified polyacrylonitrile from aqueous solution, *Chem. Technol. Indian J.*, 8 (2013) 121–127.
- [30] M.A. Abu-Saied, E.S. Abdel-Halim, M.M.G. Fouda, S.S. Al-Deyab, Preparation and characterization of iminated polyacrylonitrile for the removal of methylene blue from aqueous solutions, *Int. J. Electrochem. Sci.*, 8 (2013) 5121–5135.
- [31] F. Rozada, L.F. Calvo, A.I. Garcia, J. Martín-Villacorta, M. Otero, Dye adsorption by sewage sludge-based activated carbons in batch and fixed-bed systems, *Bioresour. Technol.*, 87 (2003) 221–230.

- [32] G. Gode, E. Pehlivan, Adsorption of Cr(III) ions by Turkish brown coals, *Fuel Process. Technol.*, 86 (2005) 875–884.
- [33] Y.-S. Ho, Effect of pH on lead removal from water using tree fern as the sorbent, *Bioresour. Technol.*, 96 (2005) 1292–1296.
- [34] M.M. Dubinin, E.D. Zaverina, L.V. Radushkevich, Sorption and structure of active carbons I. adsorption of organic vapors, *Zhurnal Fizicheskoi Khimii*, 21 (1947) 1351–1362.
- [35] N. Unlü, M. Ersoz, Adsorption characteristics of heavy metal ions onto a low cost biopolymeric sorbent from aqueous solutions, *J. Hazard. Mater.*, 136 (2006) 272–280.
- [36] M. Ajmal, R.A.K. Rao, R. Ahmad, J. Ahmad, Adsorption studies on *Citrus reticulata* (fruit peel of orange): removal and recovery of Ni(II) from electroplating wastewater, *J. Hazard. Mater.*, 79 (2000) 117–131.
- [37] A. Stolz, Basic and applied aspects in the microbial degradation of azo dyes, *Appl. Microbiol. Biotechnol.*, 56 (2001) 69–80.
- [38] B.H. Hameed, L.H. Chin, S. Rengaraj, Adsorption of 4-chlorophenol onto activated carbon prepared from rattan sawdust, *Desalination*, 225 (2008) 185–198.
- [39] M.I. Temkin, V. Pyzhev, Kinetics of ammonia synthesis on promoted iron catalysts, *Acta Physicochim. URSS*, 12 (1940) 327–356.
- [40] I.A.W. Tan, A.L. Ahmad, B.H. Hameed, Adsorption isotherms, kinetics, thermodynamics and desorption studies of 2,4,6-trichlorophenol on oil palm empty fruit bunch-based activated carbon, *J. Hazard. Mater.*, 164 (2009) 473–482.
- [41] M.J. Tempkin, V. Pyozhev, Kinetics of ammonia synthesis on promoted iron catalyst, *Acta Physicochim. URSS*, 12 (1940) 327–352.
- [42] A.U. Itodo, H.U. Itodo, Sorption energies estimation using Dubinin-Radushkevich and Temkin adsorption isotherms, *Life Sci. J.*, 7 (2010) 31–39.
- [43] M. Özacar, I.A. Sengil, A kinetic study of metal complex dye sorption onto pine sawdust, *Process Biochem.*, 40 (2005) 565–572.
- [44] Y.S. Ho, G. McKay, Pseudo-second order model for sorption processes, *Process Biochem.*, 34 (1999) 451–465.
- [45] R.-L. Tseng, Mesopore control of high surface area NaOH-activated carbon, *J. Colloid Interface Sci.*, 303 (2006) 494–502.
- [46] G. Crini, H.N. Peindy, F. Gimbert, C. Robert, Removal of C.I. Basic Green 4 (Malachite Green) from aqueous solutions by adsorption using cyclodextrin-based adsorbent: kinetic aium studies, *Sep. Purif. Technol.*, 53 (2007) 97–110.
- [47] G. McKay, The adsorption of dyestuffs from aqueous solution using activated carbon: analytical solution for batch adsorption based on external mass transfer and pore diffusion, *Chem. Eng. J.*, 27 (1983) 187–195.
- [48] W.J. Weber, J.C. Morris, Kinetics of adsorption on carbon from solution, *J. Sanitary Eng. Div. Am. Soc. Civ. Eng.*, 89 (1963) 31–59.
- [49] K. Kannan, M.M. Sundaram, Kinetics and mechanism of removal of methylene blue by adsorption on various carbons—a comparative study, *Dyes Pigm.*, 51 (2001) 25–40.
- [50] M. Sarkar, P.K. Acharya, B. Bhaskar, Modeling the adsorption kinetics of some priority organic pollutants in water from diffusion and activation energy parameters, *J. Colloid Interface Sci.*, 266 (2003) 28–32.
- [51] V.J.P. Poots, G. McKay, J.J. Healy, Removal of basic dye from effluent using wood as an adsorbent, *J. Water Pollut. Control Fed.*, 50 (1978) 926–939.
- [52] G. McKay, M.S. Otterburn, J.A. Aga, Fuller's earth and fired clay as adsorbents for dyestuffs, *Water Air Soil Pollut.*, 24 (1985) 307–322.
- [53] G.E. Boyd, A.W. Adamson, L.S. Myers, The exchange adsorption of ions from aqueous solutions by organic zeolites. II. Kinetics, *J. Am. Chem. Soc.*, 69 (1947) 2836–2848.
- [54] A.E. Ofomaja, Kinetic study and sorption mechanism of methylene blue and methyl violet onto mansonia (*Mansonia altissima*) wood sawdust, *Chem. Eng. J.*, 143 (2008) 85–95.
- [55] T.A. Khan, S. Dahiya, I. Ali, Use of kaolinite as adsorbent: equilibrium, dynamics and thermodynamic studies on the adsorption of Rhodamine B from aqueous solution, *Appl. Clay Sci.*, 69 (2012) 58–66.
- [56] G.X. Zhao, J.X. Li, X.K. Wang, Kinetic and thermodynamic study of 1-naphthol adsorption from aqueous solution to sulfonated graphene nanosheets, *Chem. Eng. J.*, 173 (2011) 185–190.
- [57] M. Alkan, Ö. Demirbaş, S. Çelikçapa, M. Doğan, Sorption of acid red 57 from aqueous solution onto sepiolite, *J. Hazard. Mater.*, B116 (2004) 135–145.